

## Supporting Information

# Multifunctional biocompatible Ni/Ni-P Nanospheres for anti-tumor “Neoadjuvant Phototherapy” cooperating photothermal therapy and photodynamic therapy

Peizhe Song <sup>a,&</sup>, Shujuan Jin <sup>b,&</sup>, Yue Cao <sup>c</sup>, Shaopeng Zhang <sup>a</sup>, Na Yin <sup>d,e</sup>, Hao Zhang <sup>d,e</sup> and Daguang Wang <sup>a,\*</sup>

<sup>a</sup> Department of Gastrocolorectal Surgery, General Surgery Center, The First Hospital of Jilin University, Changchun 130021, China

<sup>b</sup> Senior Department of General Surgery, The First Medical Center of Chinese PLA General Hospital, Fuxin Road, No. 28, Haidian District, Beijing, 100853, China

<sup>c</sup> Department of Neurosurgery, The First Hospital of Jilin University, Changchun 130021, China

<sup>d</sup> State Key Laboratory of Rare Earth Resource Utilization, Changchun Institute of Applied Chemistry, Chinese Academy of Sciences, Changchun, Jilin, 130022, P. R. China

<sup>e</sup> School of Applied Chemistry and Engineering, University of Science and Technology of China, Hefei, Anhui 230026, P. R. China

\* Correspondence: [daguangjida@163.com](mailto:daguangjida@163.com)

& These authors contributed equally to this work

## Experimental section

### Chemicals and Reagents

Nickel chloride ( $\text{NiCl}_2 \cdot 6\text{H}_2\text{O}$ ), ammonia solution ( $\text{NH}_3 \cdot \text{H}_2\text{O}$ ), sodium hypophosphite monohydrate ( $\text{NaH}_2\text{PO}_2$ ), anhydrous sodium acetate (NaAc) and potassium hydroxide (KOH) were purchased from Beijing Chemical Reagents Company (Beijing, China). Indocyanine Green (ICG) and polyethyleneimine (PEI) were bought from Shanghai Aladdin Bio-Chem Technology Company (Shanghai, China).

### Photothermal conversion efficiency of NNPP NPs

Photothermal conversion efficiency of NNPP NPs is calculated by the following equation:<sup>1</sup>

$$\theta = (T - T_{\text{surr}}) / (T_{\text{max}} - T_{\text{surr}}), \quad (1)$$

$$t = \tau_s \times (-\ln \theta), \quad (2)$$

$$hS = m_i C_i / \tau_s, \quad (3)$$

$$\eta = [ hS(T_{\max} - T_{\text{surr}}) - hS(T_{\max, \text{water}} - T_{\text{surr}}) ] / [ I(1 - 10^{-A_{808}}) ] \times 100\%. \quad (4)$$

T : temperature on cooling curve; t : time point on cooling curve;  $T_{\max}$  : equilibrium temperature;  $T_{\text{surr}}$  : ambient temperature;  $m_i$  : solution mass;  $C_i$  : specific heat capacity of solution;  $A_{808}$  : UV-vis absorption of NNPP NPs aqueous solution at 808 nm;  $\tau_s$  : the sample system time constant; h : heat transfer coefficient; S : the irradiated area; I : power density of 808 nm continuous laser;  $\eta$  : photothermal conversion efficiency.

### Thermal stability of NNPP NPs

1.0 mL of NNPP NPs aqueous solution was irradiated with 1.0 W/cm<sup>2</sup> of 808 nm continuous laser for 10 min, and then naturally cooled to room temperature. The above process is repeated four times.

### ICG loading

While stirring, 20mg of PEI was added dropwise into the aqueous solution of Ni<sub>3</sub>P-Ni (0.133mg/ml, 4mg). After stirring for 4 h, ICG (0.4mg) was added. After 4 h, the mixture was centrifuged and the supernatant was collected. The ICG loading was measured by measuring the UV-vis absorption spectra of centrifuged supernatant. The ICG loading content (LC) is calculated by the following equation:

$$\text{LC}\% = (m_{\text{total}} - m_{\text{supernatant}}) / m_{\text{total}} \times 100\%.$$

### Detection of singlet oxygen (<sup>1</sup>O<sub>2</sub>)

DI solution of SOSG (66 μL, 100 μM) and NNPIP NPs (2.0 mL, 0.2 mg/ml) was mixed together and irradiated with 808 nm laser (1.0 W/cm<sup>2</sup>) for 0 min, 2 min, 4 min, 6 min, 8 min or 10 min. Then luminescent spectra of supernatant were detected under the 448 nm excitation after centrifugation.

### Mice and cell lines

615 mice, 5 weeks of age, female, were from JKbiot. Mouse Forestomach Carcinoma (MFC) cells and 4T1 cells were purchased from Pricella. L929 cells were provided by Dr. Zhang Hao (University of Science and Technology of China).

### Cell Culture

Both MFC cells, 4T1 cells and L929 cells were seeded in Roswell Park Memorial Institute (RPMI) 1640 medium (Gibco, CA, USA) with the addition of 100 μg/mL penicillin and 100 μg/mL streptomycin (Hyclone, Logan, UT, USA), and 10% FBS (Gibco, CA, USA). And the culture circumstance is a humidified incubator (ThermoFisher) containing 5% CO<sub>2</sub> at 37°C.

### Annexin V-FITC apoptosis assay

The levels of apoptotic or necrotic cells were determined by flow cytometric analysis. After the treatment with different conditions, the medium was removed. The applied concentration of NNPIP NPs or NNPP NPs is 200 μg/ml. The applied concentration of ICG is the correspondingly loaded amount. MFC cells or 4T1 cells were illuminated by 1.0 W/cm<sup>2</sup> of 808 nm continuous laser for 5 min and further cultured. Then the MFC or 4T1 cells were washed with PBS, digested, harvested and collected by centrifugation. Subsequently, the cell pellets were washed with ice-cold PBS and resuspended in 1× binding buffer. The cell suspension was stained with Annexin V-FITC and PI. Finally, the cell samples were analyzed by flow cytometer and the percentages of apoptotic and necrotic cells were recorded. A minimum of 10,000 cells were counted.

### Mice Model

We started with an MFC cell count of about 1×10<sup>7</sup> and suspended them into PBS. And the cell suspension was implanted subcutaneously into the left hip of 615 mice and initiated therapeutic protocol in six days. Tumor volume was measured once every two days using the formula: Volume = (length × width × width)/2. And the initial tumor volume on Day 1 in each group was as follow: “Control” (219.29±16.52 mm<sup>3</sup>), “808nm” (217.52±14.92 mm<sup>3</sup>), “ICG+808nm” (222.05±15.84 mm<sup>3</sup>), “NNPP+808nm” (226.28±14.20 mm<sup>3</sup>), “NNPIP+808nm” (236.91±10.82 mm<sup>3</sup>). The animal experiments were accomplished according to the Institutional Animal Care and Use Ethical Committee guidelines at the center of the Jilin University Animal Experiment.

### In vivo treatment

Twenty mice were randomly assigned to 5 groups (n=4, in each group) and each group received different treatment by intravenous injection (i.v.). Mice in group “Control” were injected with PBS solution. Mice in group “808nm” were treated with 808 nm laser onto the tumor. Mice in group “ICG + 808 nm” were injected

with the solution of corresponding loading amount of ICG and treated with 808 nm laser onto the tumor. Mice in group “NNPP + 808 nm” were injected with 5 mg/ml of NNPP NPs and treated with 808 nm laser onto the tumor. Mice in group “NNPIP + 808 nm” were injected with 5 mg/ml of NNPIP NPs and treated with 808 nm laser onto the tumor. All of the above intravenous fluids were administered in a volume of 0.1 ml. We use the laser whose power density was 1 W/cm<sup>2</sup> to illuminate the tumor of mice for 10 min. During the treatment as Figure 5a, we recorded the body weight and tumor volume of the mice every two days. On the 15th day, we sacrificed the mice, weighed the quality of the tumors to assess the therapeutic effect and subjected the corresponding tissues and organs to HE staining .

#### **Biodistribution of NNPIP NPs**

0.1 ml of 5 mg/mL NNPIP NPs solution were injected intravenously, and the mice were sacrificed at different time points (12 hour, 24 hour and 48 hour) after injection. The tumors and organs of the mice were picked up and dissolved into 5ml of aqua regia. After the tumor and organs were completely immersed in aqua regia, the content of Mn was determined by ICP analysis.

#### **In vitro and vivo MRI**

The MRI signals of different concentrations of NNPIP NPs solution in DI were measured in vitro by utilizing a clinical MRI scanner (3.0 T). And 0.1 ml of NNPIP NPs solution was injected intravenously into untreated tumor-bearing mice to measure the intensity of MRI signals in tumors at different time points. 0-hour point represented pre-injection.

#### **In vitro and vivo PAI**

PA imaging was measured by MSOT imaging technique (MSOT inVision 128, iThera Medical GmbH, Munich, Germany). In vitro PA imaging of NNPIP NPs aqueous solution with different concentrations was measured. We injected 0.1 ml of NNPIP NPs solution intravenously into tumor-bearing mice, and the in vivo PA signals was measured before (0 hour) and after (12 hour, 24 hour and 48 hour) injection. The mice were scanned repeatedly under pulsed lasers of different wavelengths (680, 715, 750, 785, 820, 855, and 890 nm).

#### **In vivo NIR imaging**

Tumor imaging: NNPIP NPs (5 mg/mL, 0.1 ml) were injected into tumor-bearing mice by i.v., and 24h later collected the images at different time points (0, 2, 4, 6, 8, 10 min).

## **Results and discussion**

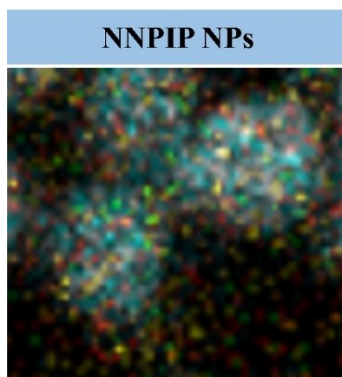


**Figure S1.** Merged elemental mapping image of NNPIP NPs including Ni, P, N, O and C.

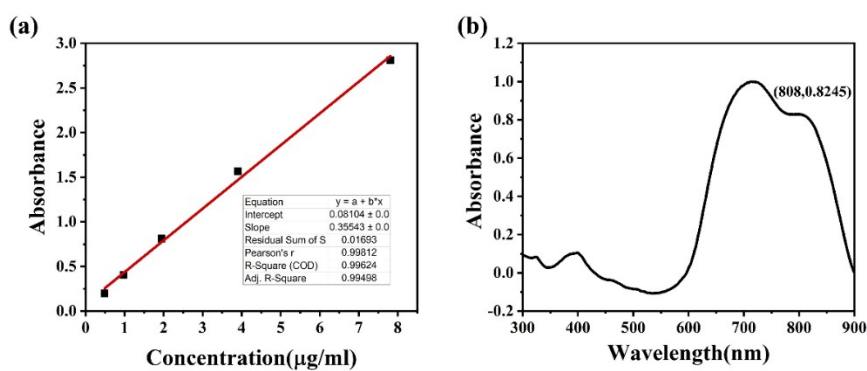


**Figure S2.** (a) The UV-vis standard curve of ICG. (b) The UV-vis absorbance spectrum of NNPIP NPs supernatant.

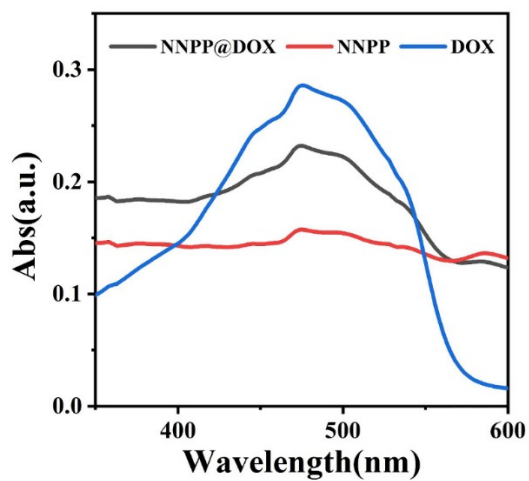


**Figure S3.** The UV-vis absorbance spectrum of DOX, NNPP and NNPP@DOX NPs.

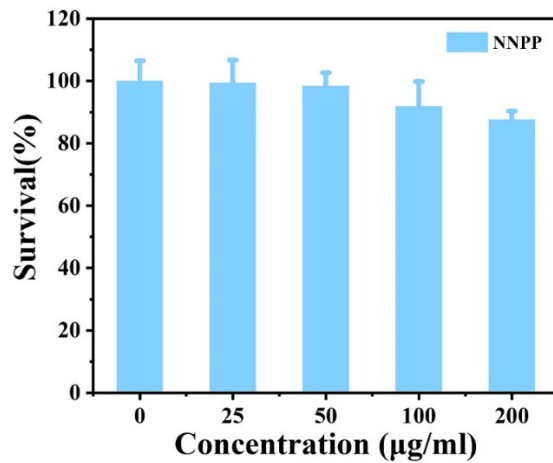


Figure S4. Cytotoxicity of NNPP NPs to 4T1 cells assessed by CCK-8 assay.

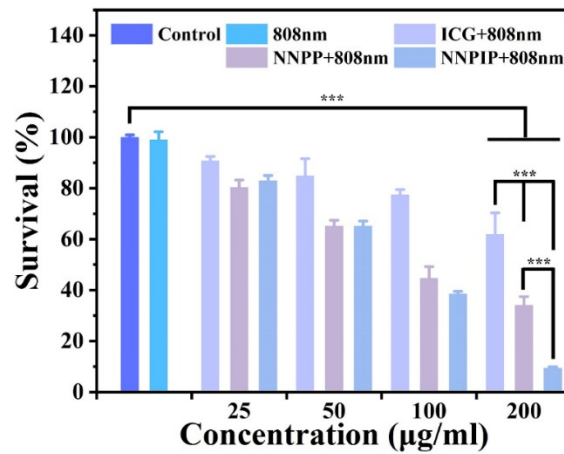


Figure S5. The cell survival rate of 4T1 cells under different conditions evaluated by CCK-8 assay. One-way ANOVA analyses were performed. \*\*P < 0.01, \*\*\*P < 0.001.

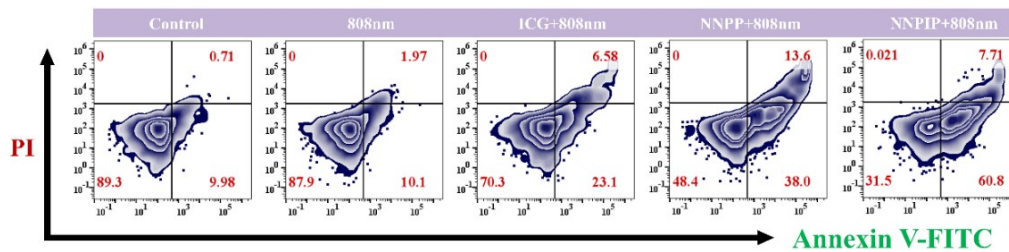
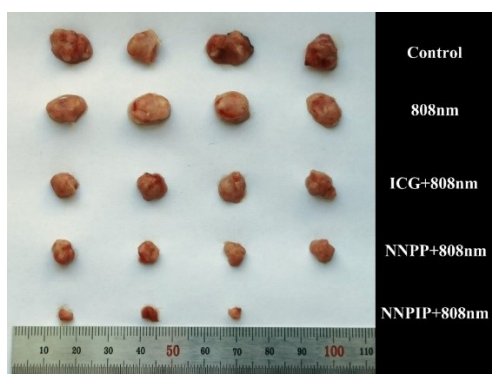
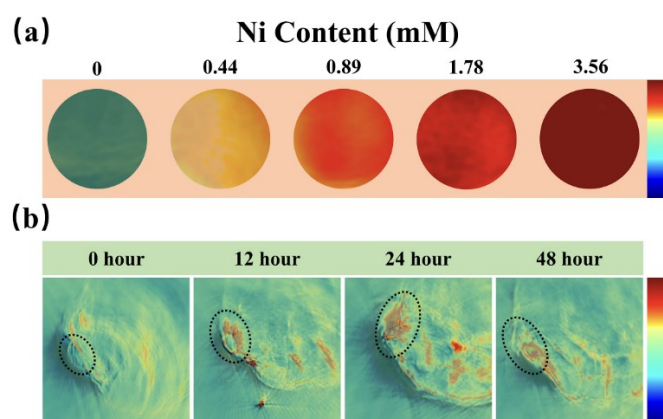


Figure S6. Apoptosis detection of 4T1 cells after incubation with different conditions evaluated by flow cytometric analysis.



**Figure S7.** The photo of tumors on Day 15 (n = 4, in each group).



**Figure S8.** (a) The strength of PAI signals of NNPIP NPs with different Ni content in vitro. (b) The PAI of tumor in vivo at at hours 0, 12, 24 and 48 after intravenous injection of NNPIP NPs.

**Table S1.** Photothermal performance of reported nanoagents.

| Materials  | Photothermal conversion efficiency ( $\eta$ , %) | Wavelength ( $\lambda$ , nm) | References      |
|--|--|------------------------------|-----------------|
| MoS <sub>2</sub> -Cys                                | 35.0   | 808 nm                       | S <sup>2</sup>  |
| PPy vesicles   | 24.2   | 808 nm                       | S <sup>3</sup>  |
| PVP-Bi   | 30.0   | 808 nm                       | S <sup>4</sup>  |
| NiPPD NPs  | 18.5   | 808 nm                       | S <sup>5</sup>  |
| 9T-PUNNC<br>(PEGylated nickel<br>nanoclusters)       | 20.93  | 1064 nm                      | S <sup>6</sup>  |
| Complex 1<br>(Ni-based metal-organic<br>framework)   | 10.75  | 660 nm                       | S <sup>7</sup>  |
| NPs [Ni <sub>4</sub> C <sub>12</sub> ]               | 26.0   | 940 nm                       | S <sup>8</sup>  |
| NiO NPs@AuNPs@Van<br>(NAV)                           | 30.0   | 808 nm                       | S <sup>9</sup>  |
| CaO <sub>2</sub> @CuS-MnO <sub>2</sub> @HA<br>(CCMH) | 37.2   | 1064 nm                      | S <sup>10</sup> |

## Notes and references

- 1 Y. Lu, P. Zhang, L. Lin, X. Gao, Y. Zhou, J. Feng and H. Zhang, *Dalton Trans.*, 2022, **51**, 4423–4428.
- 2 L. Ding, Y. Chang, P. Yang, W. Gao, M. Sun, Y. Bie, L. Yang, X. Ma and Y. Guo, *Materials Science and Engineering: C*, 2020, **117**, 111371.
- 3 L. Ruiz-Pérez, L. Rizzello, J. Wang, N. Li, G. Battaglia and Y. Pei, *Soft Matter*, 2020, **16**, 4569–4573.
- 4 P. Lei, R. An, P. Zhang, S. Yao, S. Song, L. Dong, X. Xu, K. Du, J. Feng and H. Zhang, *Advanced Functional Materials*, 2017, **27**, 1702018.
- 5 R. Yang, R. Li, L. Zhang, Z. Xu, Y. Kang and P. Xue, *J. Mater. Chem. B*, 2020, **8**, 7766–7776.
- 6 Y. Qian, J. Zhang, J. Zou, X. Wang, X. Meng, H. Liu, Y. Lin, Q. Chen, L. Sun, W. Lin and H. Wang, *Theranostics*, 2022, **12**, 3690–3702.
- 7 X. Pei, L. Dang, T. Zhang, T. Chen, F. Ren and S. Liu, *Catalysts*, 2022, **12**, 777.
- 8 M. Ciancone, K. Mebrouk, N. Bellec, C. L. Goff-Gaillard, Y. Arlot-Bonnemains, T. Benvegnu, M. Fourmigué, F. Camerel and S. Cammas-Marion, *J. Mater. Chem. B*, 2018, **6**, 1744–1753.
- 9 T. Du, J. Cao, Z. Xiao, J. Liu, L. Wei, C. Li, J. Jiao, Z. Song, J. Liu, X. Du and S. Wang, *Journal of Nanobiotechnology*, 2022, **20**, 325.
- 10 C. Huang, B. Lin, C. Chen, H. Wang, X. Lin, J. Liu, Q. Ren, J. Tao, P. Zhao and Y. Xu, *Advanced Materials*, 2022, **34**, 2207593.